

# Study on the Formation Mechanism and Sinterability of $\text{La}_{1-x}\text{Sr}_x\text{CoO}_{3-\delta}$ ( $x = 0.1 - 0.3$ ) Prepared by Mechanical Activation

GEORGETA VELCIU<sup>1</sup>, ADELINA CARMEN IANCULESCU<sup>2\*</sup>, ALINA MELINESCU<sup>2</sup>, VIRGIL MARINESCU<sup>1</sup>, MARIA PREDA<sup>2</sup>

<sup>1</sup> National Research & Development Institute for Electrical Engineering ICPE-CA, 313, Splaiul Unirii, 030138, Bucharest, Romania

<sup>2</sup> University Politehnica of Bucharest, Faculty of Applied Chemistry and Materials Science, 313 Splaiul Independentei, 060042, Bucharest, Romania

*In this work it was studying evolution of the reactions that occur at the formation of  $\text{La}_{1-x}\text{Sr}_x\text{CoO}_{3-\delta}$  from mixtures of  $\text{La}_2\text{O}_3$ ,  $\text{Co}_3\text{O}_4$  and  $\text{SrCoO}_3$ , prepared by mechanical activation. It was found that distributions of the particles sizes after mechanical activation are unimodal and narrow. Thermal analysis shows that the reactions that occur under the temperature of  $1000^\circ\text{C}$  are dissociation reactions of the raw materials or of intermediate compounds formed in the process of mechanical activation. The first compound found, starting from  $1000^\circ\text{C}$  was  $\text{LaCoO}_3$ , whereas  $\text{Co}_3\text{O}_4$  and  $\text{CoO}$  were observed as secondary phases. By measuring the apparent density of the thermally treated samples, a good tendency to sintering was noticed. SEM images and EDX analyses allowed to highlight the high sinterability of the samples.*

*Key words:  $\text{LaSrCoO}_3$  solid solutions, mechanical activation, RDX, SEM, thermal analyses*

$\text{La}_{1-x}\text{Sr}_x\text{CoO}_{3-\delta}$  (LSC) solid solutions are intensely studied, because of the high solid state mobility of oxygen ions, which makes them useful for many applications such as catalysts, separators membranes, gas sensors and electrodes for electrochemical devices. The aliovalent incorporation of  $\text{Sr}^{2+}$  ions onto  $\text{La}^{3+}$  sites in the  $\text{LaCoO}_3$  lattice induces significant structural changes and modifications of electrical properties that leads to diversifying of the applications of these materials. The study of the phase diagram of the La-Sr-Co-O system showed the presence of the binary  $\text{Sr}_2\text{Co}_2\text{O}_5$  and  $\text{LaCoO}_3$  compounds and of several types of solid solutions [1]. In the binary Sr-Co-O system the  $\text{Sr}_2\text{Co}_2\text{O}_5$  compound is stable up to  $1227^\circ\text{C}$  when it dissociates in the presence of the liquid phase [2]. It has a hexagonal structure and it may be stabilized at room temperature as a function of the degree of ordering of oxygen vacancies.  $\text{LaCoO}_3$  belonging to the binary La-Co-O system exhibits rhombohedral structure [2-5]. The substitution of  $\text{La}^{3+}$  with  $\text{Sr}^{2+}$  in the  $\text{LaCoO}_3$  network, leads to the formation of oxygen vacancies as compensating defects determined by the difference in electric charge between the two cations. Another compensation mechanism for maintaining electro neutrality involves the modification of the cobalt valence that can vary from 2+ to 4+ [6]. For this reason  $\text{La}_{1-x}\text{Sr}_x\text{CoO}_{3-\delta}$  exhibits a mixed conductivity through both oxygen ions and either electrons or holes.

Several preparation methods, as solid state reaction [7], combustion [8-11], mechanical activation [5], etc., were proposed in order to obtain  $\text{La}_{1-x}\text{Sr}_x\text{CoO}_{3-\delta}$ . Preparation by mechanical activation is presently extensively studied because it is simple and leads to very fine powder [12]. In the case of the mixtures prepared by mechanical activation different changes occur in raw materials, i.e. the decrease of particle size and the increase of the specific surface area, local plastic deformation and changes of crystal lattice, all leading to the increase of chemical reactivity and to the modification of solid-state reaction mechanisms [13-15]. Particles resulted finally from mechanical activation are uniform in terms of size and less crowded [16].

The aim of this work is to study the formation mechanism of the  $\text{La}_{1-x}\text{Sr}_x\text{CoO}_{3-\delta}$  solid solutions and the sinterability of their related ceramics thermally treated in different conditions.

## Experimental part

### Sample preparation and experimental details

Three raw materials of high purity, i.e.  $\text{La}_2\text{O}_3$ ,  $\text{SrCO}_3$  and  $\text{Co}_3\text{O}_4$  were used in order to prepare  $\text{La}_{1-x}\text{Sr}_x\text{CoO}_{3-\delta}$  ( $x = 0.1, 0.2, 0.3$ ) solid solutions. The samples were denoted LSC-1, LSC-2 and LSC-3, respectively. The mixtures of raw materials were prepared by mechanical activation in a Pulverisette mill, for 10 h, in ethanol as a wetting medium. The details of this method were given in ref [5]. The particle size distributions of the powders were determined by means of a Brookhaven 90 Plus laser particle size analyzer and the results were represented in the differential form. The curves obtained were characterized by modal diameter in nm and relative width expressed as a percentage [17]. The thermal treatment behaviour was studied by thermal analysis methods as DSC, TG and DTG, using a 449 F3 Jupiter STA equipment. From the as-prepared powders, discs with a diameter of 10 mm were obtained by pressing at 100 MPa. These were thermally treated at temperatures ranged between 1000 and  $1300^\circ\text{C}$  with a plateau of two hours. Apparent density of the samples was determined by the Archimedes method. Phase compositions were examined by X-ray diffraction, with a Shimadzu 6100 diffractometer, using Ni-filtered  $\text{CuK}$  ( $\lambda = 1.5402\text{\AA}$ ). The microstructure of the ceramic samples was observed by scanning electron microscopy with an Auriga FEG-SEM FIB microscope.

## Results and discussions

### Study of the powders

The particle size distributions are shown in figure 1 (a-c). It was found in all cases a unimodal distribution that was characterized by modal diameter (MD) and width relative distribution (Wr) calculated from experimental measurements. The modal diameter for all samples is within submicron range, presenting small variations by

\* email: a\_ianculescu@yahoo.com

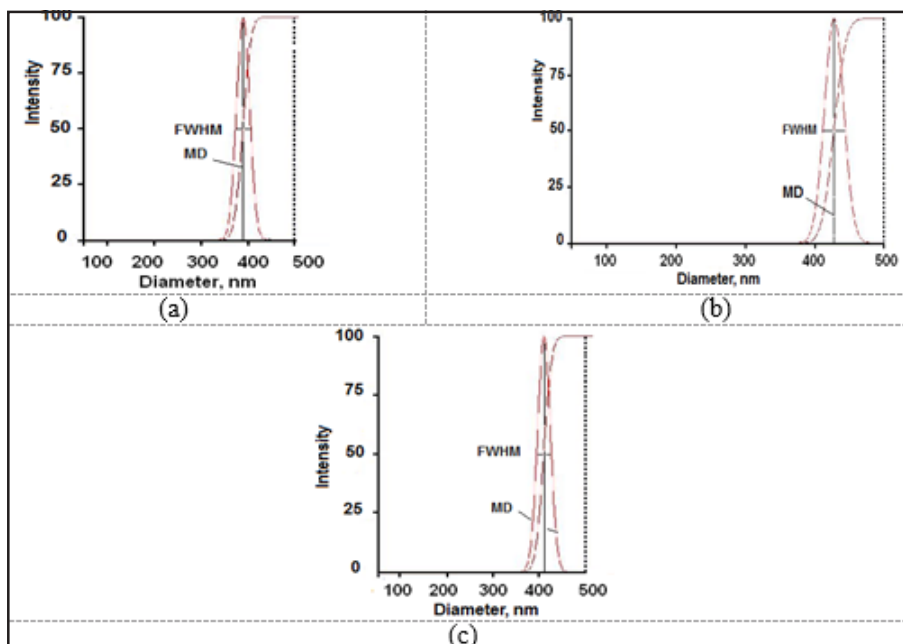


Fig. 1. The distributions of grain sizes from mixtures by mechanical activation prepared for 10 h: (a) LSC-1 (MD-387 nm;  $W_r=3.2\%$ ); (b) LSC-2 (MD-428 nm;  $W_r=3.7\%$ ); (c) LSC-3 (MD-406 nm;  $W_r=3.7\%$ )

changing the quantitative ratio of raw materials. The width of relative distributions exhibits very low values, indicating a narrow range of particle sizes of the powder mixtures. The full width at half maximum (FWHM) are also shown in figure 1 (a-c).

The thermal behaviour of mixtures was determined by thermal analyses. Thus, in figure 2 the thermal analysis curves recorded during the heating of the sample LSC-1 are presented.

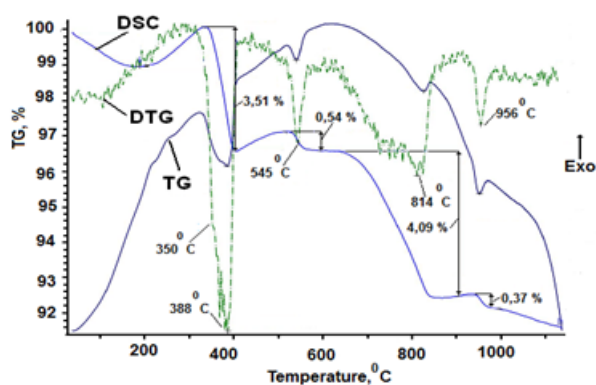


Fig. 2. Thermal analysis curves of sample LSC-1

It was found on the DSC curve the presence of four endothermic effects, all accompanied by mass loss. From the previous obtained results, lanthanum oxide was partial hydrated and carbonated into the process of grinding [5], which explains the presence of the first endothermic effect having two maxima at temperatures of 350 and 388°C on DTG curve. The effect from 350°C is the removal of water from lanthanum hydroxide with  $\text{LaOOH}$  formation. The effect which occurs at 388°C may be assigned the removal of water from a hydroxy-carbonated compound and the formation  $\text{La}_2\text{O}_2\text{CO}_3$  as has been shown in [5].

The effect centered at 545°C corresponds to removal of water from  $\text{LaOOH}$  with  $\text{La}_2\text{O}_3$  formation. Then follows a complex effect, centered at 814°C, which includes the elimination of carbon dioxide from the  $\text{La}_2\text{O}_2\text{CO}_3$ , and partly from  $\text{SrCO}_3$ , as well as elimination of oxygen from  $\text{Co}_3\text{O}_4$ , after partial reduction of ions  $\text{Co}^{3+}$  in  $\text{Co}^{2+}$ , according to the reaction  $\text{Co}_3\text{O}_4 \rightarrow 3\text{CoO} + 1/2\text{O}_2$ . The fact that this effect is due to multiple processes of decomposition is evidenced especially by complex characteristic feature, registered on the DTG curve.

In previous work it showed that the carbon dioxide is eliminated in two stages at different temperatures. It can be noted and in this case that the effect at 956°C is due to the second stage of elimination of  $\text{CO}_2$  from network of residual strontium carbonate in the mixture. It should be noted that all temperatures are lower than the corresponding to pure raw materials. Similar effects are also found for the sample LSC-2 (fig. 3).

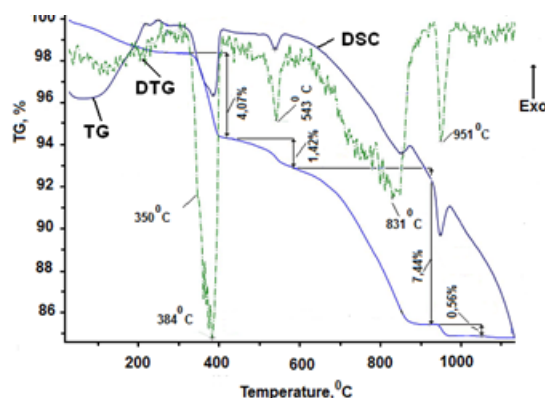


Fig. 3. Thermal analysis curves of sample LSC-2

The loss of mass of which is more important (7.44%) for LSC-2 sample in the range of 650 – 850°C in comparison to the case of the LSC-1 sample (4.09%) is due to the higher proportion of the  $\text{SrCO}_3$  present in the mixture which involves the release of high amounts of the  $\text{CO}_2$  during the decomposition. The increased amount of strontium determines a more clear evidence of the processes of decomposition, as shown by the LSC-3 sample (fig. 4).

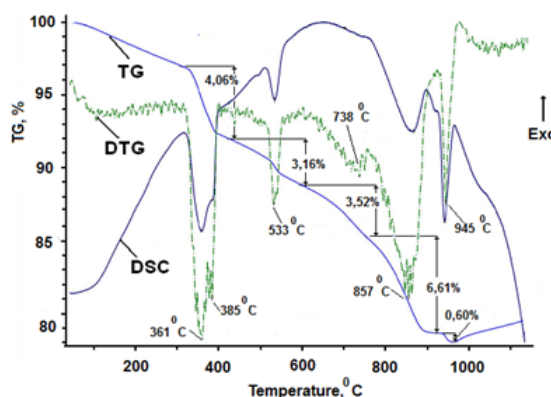


Fig. 4. Thermal analysis curves of sample LSC-3

Thus, besides the three effects at low temperatures 361, 385 and 533°C it was found a complex effect having two maxima at 738 and 857°C, respectively. The first effect is easily noticeable on the DTG curve and is the result of the  $\text{La}_2\text{O}_3$  endothermic decomposition. The second effect can be attributed to the processes which are similar to decomposition of  $\text{SrCO}_3$ . The final endothermic effect, at the temperature of 945°C, can be attributed to last stage of  $\text{CO}_2$  elimination from  $\text{SrCO}_3$  residual network (fig. 4). From the obtained results it follows that the processes occurring at the thermal treatment of these samples are very complex, and show only phenomena of dissociation of raw materials or of intermediate compounds formed during the reaction.

### Study on sintered samples

#### Ability to sintering

The tendency at sintering was studied for the three samples and the variation of the apparent density for ceramics versus thermal treatment temperature is given in figure 5.

The sample LSC-1 thermally treated exhibits volume inconstancy at temperatures of 1100 and 1150°C. This can occur due to the presence of a small amount of free lanthanum oxide, which is highly reactive, relative to water. This oxide could not be identified by X-ray diffraction, either because of its small amount, below the detection limit of the apparatus, or because of its predominantly amorphous nature which hinders its identification by XRD. At higher temperatures than 1150°C the LSC-1 sample has a good tendency to sinterability. One can notice a monotonous increase of the apparent density values for all three samples with the increase of thermal treatment temperature up to 1250°C, indicating a high sinterability of these ceramics.

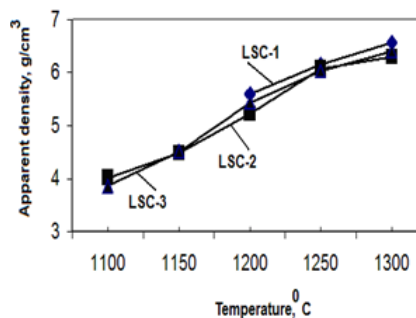


Fig. 5. Variation of density as a function of temperature for the sintered samples

#### Phase composition

The samples thermally treated at temperatures ranged between 1000 and 1250°C were analyzed by X-ray diffraction. The XRD patterns recorded at room temperature for the LSC-1 sample thermally treated at various temperatures with a constant plateau of 2 h are given in figure 6.

The formation of a well-crystallized solid solution, with the perovskite structure of  $\text{LaCoO}_3$ , was already noticed in the case of the ceramic sample thermally treated at 1000°C. Alongside  $\text{LaCoO}_3$  which represents the majority phase  $\text{Co}_3\text{O}_4$  was also identified as secondary phase by its main diffraction lines up to 1100°C (fig. 6 (a)). Starting the heating from 1000°C up to 1200°C, the diffraction lines of  $\text{CoO}$  were also identified. This sample becomes single phase after thermal treatment at 1250°C, when it consists only of a perovskite solid solution, with rhombohedral structure (fig. 6 (b)). XRD results for sintering the LSC-2 sample are shown in figure 7. The XRD patterns of LSC-2 sample thermally treated under the same conditions, present the specific lines of  $\text{Co}_3\text{O}_4$  and  $\text{CoO}$  up to the temperature of 1150°C (fig. 7(a)). The LSC-2 sample thermally treated at 1200 and 1250°C is monophasic as is shown in the figure 7 (b).

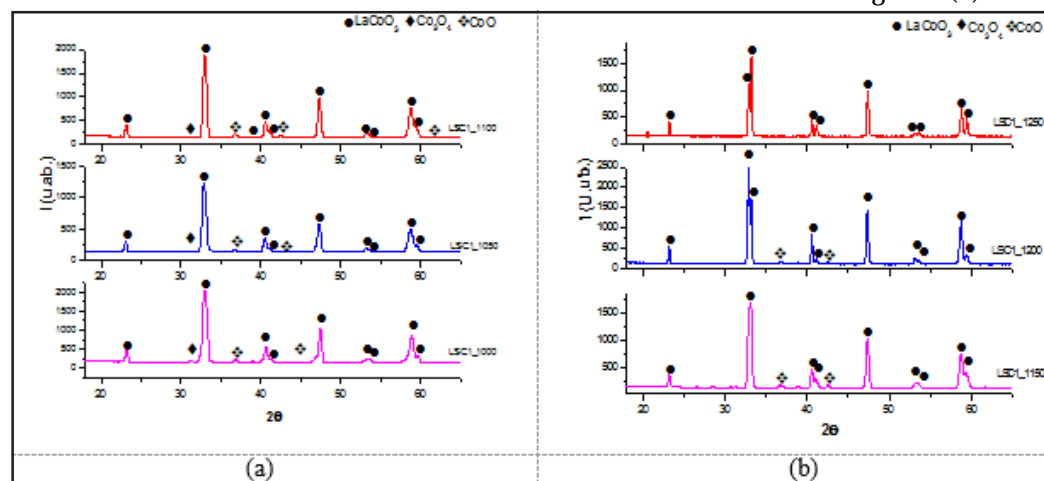


Fig. 6. XRD patterns for the ceramic LSC-1 sample thermally treated at: (a) 1000, 1050, 1100°C and (b) 1150, 1200, 1250°C

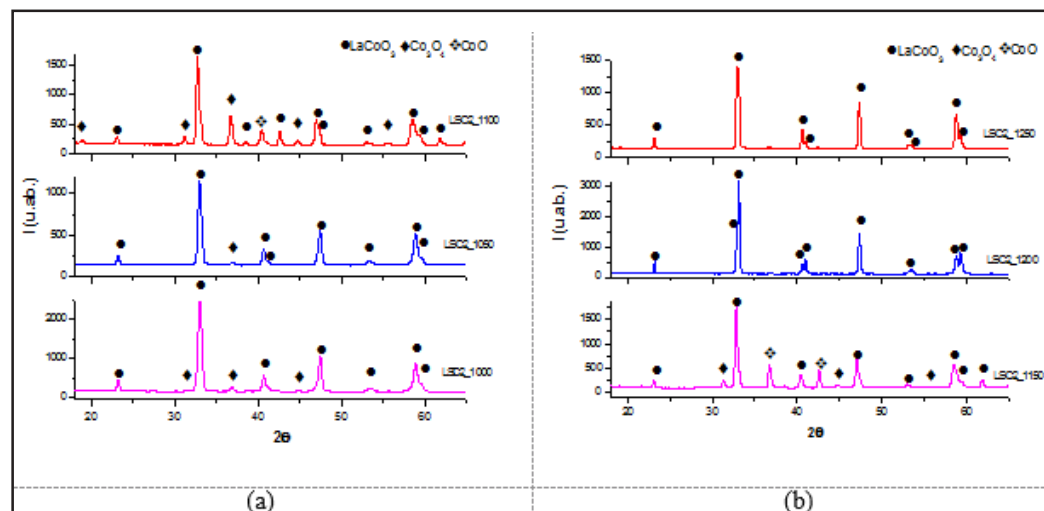


Fig. 7. XRD patterns for the ceramic LSC-2 sample thermally treated at: (a) 1000, 1050, 1100°C and (b) 1150, 1200, 1250°C

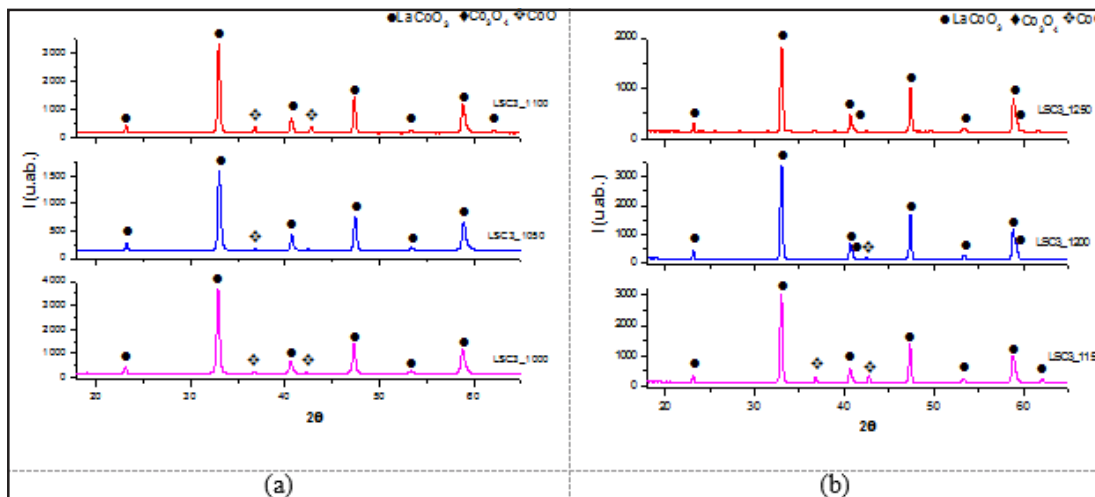


Fig. 8. XRD patterns for the ceramic LSC-3 sample thermally treated at: (a) 1000, 1050, 1100°C and (b) 1150, 1200, 1250°C

The same trend was maintained for the sintering of LSC-3 sample, as figure 8 shows. Thus, between 1000 and 1200°C it consists of two phases, *i.e.* the major  $\text{LaCoO}_3$  perovskite and the secondary  $\text{CoO}$  phase and becomes a single phase after the thermal treatment at 1250°C (fig. 8 (a), (b)).

From the performed studies it results that LSC-1 ceramics has clearly rhombohedral structure at 1250°C. The other two ceramics samples LSC-2 and LSC-3 have a cubic structure with tendency to rhombohedral deformation.

#### Microstructure

The microstructures of LSC samples, examined by scanning electron microscopy, are presented in figure 9.

The SEM image of the sample LSC-1 thermally treated at 1250°C shows the presence of polyhedral grains of sizes that ranged between 0.5 - 2  $\mu\text{m}$ , belonging to the solid solution formed during the thermal treatment process. It can be observed grains of  $\text{Co}_3\text{O}_4$  that are in a process of transformation (fig. 9 (a)). These could be not identifying by XRD due to the reduced amount. Figures 9 (b) and 9(c) shows the SEM images of the samples LSC-2 and LSC-3, respectively, where the same type of grains were observed. In the case of all the ceramics analyzed, the presence of the continuous and well-defined grain boundaries, the perfect triple junctions, as well as the absence of any type of porosity indicate an advanced densification, proving a high sinterability of the LSC ceramics derived from mechanically activated powdered mixtures.

The figure 10 shows the variation of elemental composition with distance obtained from EDX analysis inside of LSC-1, LSC-2 and LSC-3 samples.

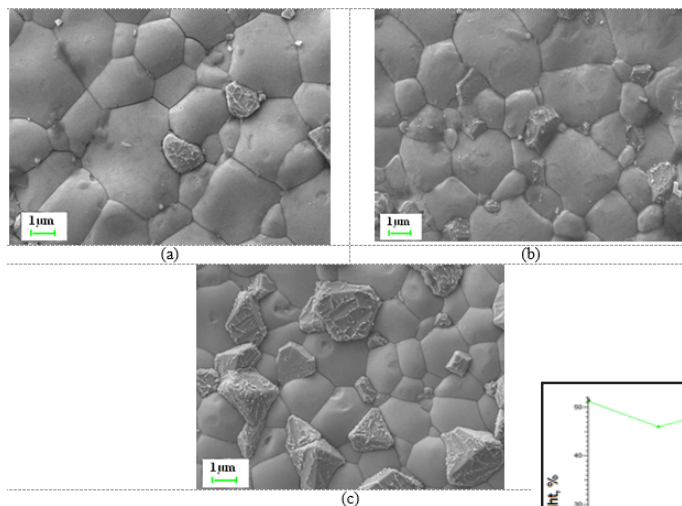


Fig. 9. SEM images for samples thermally treated at 1250°C, captured at 20.000 X (a) LSC-1; (b) LSC-2 and (c) LSC-3

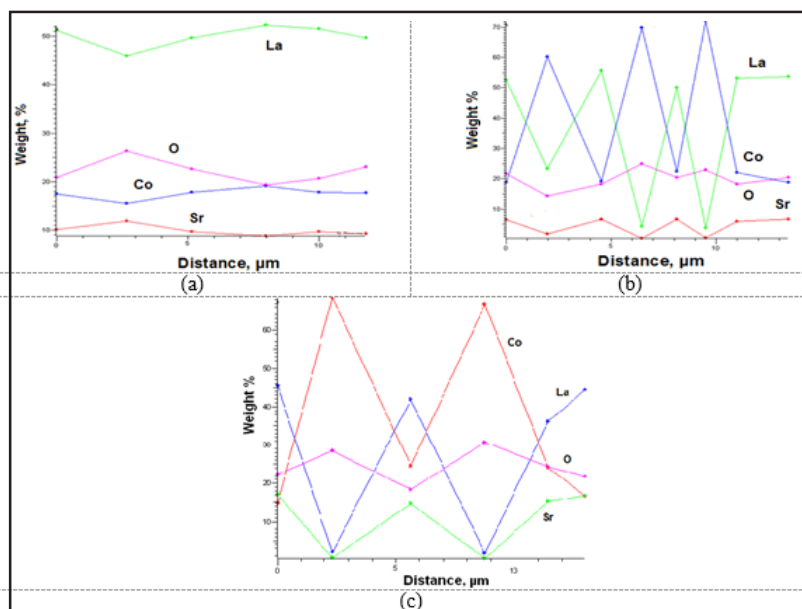


Fig. 10. Chemical composition inside of LSC samples by EDX analysis; (a) LSC-1; (b) LSC-2; (c) LSC-3



Using EDX analysis of the granules it was found that the LSC-1 is a homogeneous solid solution, meaning that it is located within the limits of solubility between  $\text{SrCoO}_3$  and  $\text{LaCoO}_3$  (fig. 10 (a)). This confirms the results previously published [1] which show that between is a limited solubility between these components. For the other two samples LSC-2 and LSC-3 was observed the presence of two types of grains: some larger grains, which are a solid solution and other smaller grains corresponding to pure  $\text{CoO}$ . This shows that the two compositions are located outside the limits of solubility. Unfortunately, the cobalt oxide could not be identified by X-ray diffraction, in the samples thermally treated at  $1250^\circ\text{C}$ , because its quantity is reduced below the limit of detection of the device or it has not the necessary degree of crystallinity.

## Conclusions

In this work the evolution of the mechanical activation reactions leading to  $\text{La}_{1-x}\text{Sr}_x\text{CoO}_{3-\delta}$  ( $x = 0.1 - 0.3$ ) formation, which occur during the heating of the powdered mixtures of  $\text{La}_2\text{O}_3$ ,  $\text{Co}_3\text{O}_4$  and  $\text{SrCO}_3$  was studied. It was found that the decomposition processes of raw materials and intermediates, as well as the formation of the skeleton of the perovskite phase taken below  $1000^\circ\text{C}$ . The increase of the Sr content in the powdered mixture induces, in the temperature range of  $650-900^\circ\text{C}$ , an increasingly more accentuated tendency of formation of individual compounds, *i.e.*  $\text{LaCoO}_3$  and  $\text{Sr}_2\text{Co}_2\text{O}_5$ . The formation of the unique  $\text{La}_{1-x}\text{Sr}_x\text{CoO}_3$  solid solution in the temperature range of  $950 - 1000^\circ\text{C}$  is the result of the inter-diffusion processes of  $\text{La}^{3+}$  and  $\text{Sr}^{2+}$  species originating from the two networks.

Single phase ceramics were obtained after thermal treatment at  $1250^\circ\text{C}$  for 2 hours. The high values of apparent density and the microstructural compactness of the single phase LSC samples indicated their high sinterability.

## References

1. CEREPANOV, V.A., GAVRILOVA, L.Ya, BARKHATOVA, L.Yu, VORONIN, V.I. TRIFONOVA, M.V., BUKHNER, O.A., Ionics **4**, 1998, p. 309 -315
2. JANKOVSKY, O., SEDMIDUBSKY, D., VÍTEK, J., SIMEK, P., SOFER, Z., J. Eur. Ceram. Soc. **35**, 2015, p. 935-940
3. HARON, W., WISITSORAAT, A., WONGNAWA, S., Int. J. Chem. Eng. Appl., 5, no. 2, 2014, p. 123-129
4. VELCIU, G., MELINESCU, A., MARINESCU, V., PREDA, M., Ceram. Int. **41**, 2015, p. 6876-6881
5. WANG, Z. L.J., YIN, S., Philosophical Magazine B, **77**, no. 1, 1998, p. 49-65
6. ANZAI, M., KAWAKAMI, H., SAITO, M., YAMAMURA, H., IOP Conf. Series: Mater. Sci. Eng., **18**, 2011, p. 142005
7. SITTE, W., BUCHER, E., PREIS, W., Solid State Ionics **154- 155**, 2002, p. 517- 522
8. MUKASYAN, A.S., COSTELLO, C., KATHERINE, P., SHERLOCK, LAFARGA, D., VARMA, A., Sep. Purif. Technol., **25**, 2001, p. 117-126
9. PERIANU, E.A., GORODEA, I.A., PRIHOR, F., MITOSERIU, L., IANCULESCU, C.A., IORDAN, A.R., PALAMARU, M.N., Rev. Chim. (Bucharest), **61**, no. 3, 2010, p. 242-244
10. PERIANU, E.A., GORODEA, I.A., GHEORGHIU, F., SANDU, A.V., IANCULESCU, A.,C., SANDU, I., IORDAN, A., R., PALAMARU, M., N., Rev. Chim. (Bucharest), **62**, no. 1, 2011, p. 17-20
11. SURYANARAYANA, C., Prog. Mater. Sci. **46**, 2001, p. 1-184
12. AVVAKUMOV, E.G., KARAKCHIEV, L.G., Chem. for Sustainable Develop., **12**, 2004, p. 287-291
13. SOMPECH, S., SRION, A., NUNTIYA, A., Sci. Asia **38**, 2012, p.102-107
14. ZHANG, Q., NAKAGAWA, T., SAITO, F., J. Alloys Compd. **308**, 2000, p. 121-125
15. KALIAGUINE, S., VAN NESTE, A., SZABO, V., GALLOT, J.E., BASSIR, M., MUZYCHUK, R., Appl. Catal., A: General **209**, 2001, p. 345-358
16. WU, H., LI, Q, J. Eur. Ceram. Soc., **1**, no.2, 2012, p. 130-137
17. WEINER, B. B., Brookhaven Instruments Corporation White Paper, 2011, p.1-3

Manuscript received: 7.10.2016